Denoising CT Images using wavelet transform

Lubna Gabralla
Faculty of Computer Science & Information Technology
Sudan University of Science &Technology
Khartoum, Sudan

Marwan Zaroug
Department of Computer Science,
College of science and arts of Baljurashi, Albaha University
Albaha, Kingdom of Saudi Arabia

Hela Mahersia
Department of Computer Science,
College of science and arts of Baljurashi, Albaha University
Albaha, Kingdom of Saudi Arabia

***Abstract*— Image denoising is one of the most significant tasks especially in medical image processing, where the original images are of poor quality due the noises and artifacts introduces by the acquisition systems. In this paper, we propose a new image denoising scheme by modifying the wavelet coefficients using soft-thresholding method, we present a comparative study of different wavelet denoising techniques for CT images and we discuss the obtained results. The denoising process rejects noise by thresholding in the wavelet domain. The performance is evaluated using Peak Signal-to-Noise Ratio (PSNR) and Mean Squared Error (MSE). Finally, Gaussian filter provides better PSNR and lower MSE values. Hence, we conclude that this filter is an efficient one for preprocessing medical images.**

Keywords*— Computed Tomography; Discrete wavelet transform; Lung cancer; Thresholding

I. INTRODUCTION

Despite the advances in oncological care, lung cancer remains the largest cause of death both worldwide and within the Kingdom of Saudi Arabia with an overall 5-year survival rate of only 15%. According to GLOBOCAN 2012 [7][8][23], lung cancer accounts 2 million deaths annually.

Recently, In KSA, the prevalence of lung cancer has increased significantly in the recent years; this is, mainly attributed to the increased incidence of smoking among men and students. The survival of patients is closely correlated to the stage of the detected lung cancer. Obviously, early detection of cancerous pulmonary nodules should improve a patient's chances for survival.

Computed tomography (CT) is the most commonly used diagnosis technique for detecting small pulmonary nodules because of its sensitivity and its ability to visualize a complete three-dimensional structure of the human thorax. It basically uses x-rays to obtain structural and functional information about the human body. An example of lung CT images is given in Figure 1.

However, the CT image quality is influenced by the radiation dose since it increases with the significant amount of radiation dose. Unfortunately, this increases the amount of x-rays being absorbed by the human body and increases the chances of cancer [15]. On the contrary, we need to reduce the radiation dose and this leads to noisy CT images. The presence of noise gives spotted images with blurred appearance [1].

Fig. 1: An example of lung CT image from ELCAP databse

Thus, recovering an original image from noisy image remains a challenging problem that has received an increasing attention in recent years [15]. The recovering can be accomplished by image denoising, a process of estimating the original image from an image that has been contaminated by noise degradation [1]. Different methods have been proposed in literature for denoising lung CT images [18][23]. In [9], the authors proposed a low-pass Gaussian filter to improve the original CT images. This filter was also used in the work of Gurcan et al. [12], Lin and Yan [16], and Lin et al. [17]. Gaussian smoothing filters were employed by Pu et al. [20], Wei et al. [24], Gori et al. [10], and Retico et al. [21] to eliminate the image artifacts. In [14], Kim et al. used median filters to reduce noise. Also, 3D multi-scale filters were used in [22] to enhance lung nodules.

These traditional methods are restricted to the analysis of spatial interactions over relatively small neighborhoods on a single scale [19]. Nevertheless, other methods based on multi-resolution analyses and wavelet transforms, become more effective because of their capability to capture the signal details in different scales [15][19].

However, to our knowledge, only few works in literature considered the wavelet approach to denoise CT lung images [2][3]. In [2], the authors propose a fusion algorithm based on wavelet transform and canny operator to detect image edges, which may reduce the noise and obtain the continuous and distinct edges, whereas in [3], the authors combine Curvelet transformation with Monte-Carlo algorithm. Firstly, CT image's Curvelet decomposition is processed, then, Monte-Carlo algorithm is used to estimate high frequency coefficients.

In this paper, we propose an efficient noise reduction technique for CT images using wavelet-based thresholding. The proposed technique consists of two different stages of processing, wavelet transformation and thresholding.

This paper is organized as follows: In Section 2, a brief introduction to wavelet transform is given. The proposed denoising system is explained in Section 3. In Section 4, experimental results for various type of noise are discussed in detail. Finally, concluding remarks are given in Section 5.

II. DISCRETE WAVELET TRANSFORM

Wavelets are functions generated from one single function Ψ by dilations and translations. The basic idea of the wavelet transform is to represent any arbitrary function as a superposition of wavelets. Any such superposition decomposes the given function into different scale levels where each level is further decomposed with a resolution adapted to that level [19]. The translated and dilated wavelet functions derived from the mother wavelet Ψ are given by equation (1):

$$\Psi_{a,b}=\frac{1}{\sqrt{a}}\Psi(\frac{t-b}{a}) \text{ with } a\neq 0 \qquad (1)$$

Where a is the scale coefficient and b is the translation coefficient. Thus, the wavelet transform of the signal x(t) is given by:

$$C_{a,b}=\int_{-\infty}^{+\infty} x(t).\Psi_{a,b}(t)\ dt \qquad (2)$$

Where the function Ψa,b must be square integrable and must have compact support.

By applying DWT to an image, the image is decomposed into four sub-bands as shown in Fig. 1(a). The sub-bands labeled LH1, HL1 and HH1 represent the finest scale wavelet coefficients, also called detail images while the sub-band LL1 corresponds to coarse level coefficients, also called approximation image. To obtain the next coarse level of wavelet coefficients, the sub-band LL1 alone is further decomposed and sampled. This results in two level wavelet decomposition as shown in Fig. 1(b). To obtain the next decomposition, LL2 will be used. This process continues until the final scale is reached.

The basic principle of denoising by wavelets was first proposed by E.-L Donoho in [4-6], where he thresholds the wavelet coefficients to zero if their values are below a certain threshold.

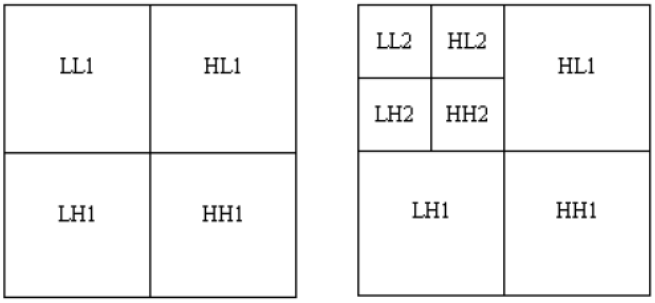

Fig. 2: the 2 level discrete wavelet decomposition for an image, from [19]

According to the noise model, a variety of threshold choosing methods can be mainly divided into four threshold selection rules [11] that are as follows:

A. *Universal Thresholding*

Universal threshold is the default method and yields the largest threshold. This type of global thresholding method was developed by [4] and the threshold value is given in equation (3) as :

$$T_{Donoho}=\hat{\sigma}\sqrt{2\log n} \qquad (3)$$

Where n is the sample size and $\hat{\sigma}$ is an estimate of the noise level σ.

B. *Heursure Thresholding*

Mixed rule is a mixture of the two previous rules: Rigrsure and universal threshold. First step calculates the variables A and B according to the system of Eq. (4)

$$\begin{cases} A=\dfrac{\sum_{i=1}^{n}|x|^2-n}{n} \\ B=\sqrt{\dfrac{1}{n}\left[\dfrac{\log n}{\log 2}\right]^3} \end{cases} \qquad (4)$$

If A is less than B the universal form threshold is as Eq. (3) is used, else threshold selection rule based on Rigrsure is adopted. A and B are defined by [11].

C. Minimax *Thresholding*

A fixed threshold selected to obtain minimum of maximum performance for mean square error against an ideal procedure.

The minimax principle is used in statistics in order to find a good estimator. The algorithm of the threshold selection is :

$$T = 0.3936 + 0.1829 \frac{\log n}{\log 2} \quad (5)$$

D. Hard and Soft thresholding

There are two thresholding methods common used the hard-threshold function which selects all wavelet coefficients that are greater than the given threshold T and sets the others to zero as shown in Eq. (6) below:

$$x_H = \begin{cases} 0 & \text{if } |x| \le T \\ x & \text{if } |x| > T \end{cases} \quad (6)$$

The other popular alternative is the soft-threshold function [13] (also called the shrinkage function) which shrinks the wavelet coefficients by T towards zero. This type of threshold is defined by Eq. (7)

$$x_S = \begin{cases} 0 & \text{if } |x| \le T \\ \text{sgn}(x)(|x| - t) & \text{if } |x| > T \end{cases} \quad (7)$$

In the next part, we calculate a new threshold function that we test for both soft and hard denoising algorithms.

III. Proposed Denoising Technique for CT Images

We modify the thresh value given by equation (3) by adding a corrective term that takes into account the variation in the computed tomography images. The new threshold function Tnew is calculated using the following equation:

$$T_{new} = \hat{\sigma} \sqrt{2 \log n - 8 \left(\frac{\sigma 1(x)}{\mu(x)}\right)} \quad (8)$$

Where n is the sample size, $\hat{\sigma}$ is an estimate of the noise level σ, σ1 and μ are respectively, the variance of the and the mean of the input noisy image.

Then we apply this new thresh T_{new} in both equations (6) and (7).

The proposed denoising scheme is explained in Figure 3.

IV. Results and Discussion

In our experiments, we have taken several gray scale images taken from ELCAP database, each of size 512 × 512. Noises tested in this work are the gaussian noise and the speckle noise. The noise levels are taken as 10, 20, 30 and 50. The wavelets tested in our experiments are: Daubechies, Haar, Symlet and Coifflet.

The results are compared with the universal threshold using both soft and hard threshold rules. The objective quality of the reconstructed image is measured by peak signal to noise ratio. The results are given in Table 1, Table 2, Figure 5. and Figure 6. It is evident from Table 1 and Table 2. that our proposed scheme outperforms the universal thresholding algorithm specially for lung CT images, for all values of noise levels considered in experiments. The robustness of the modified proposed thresh over the universal one proposed in [4] can be proved from Figure 4.

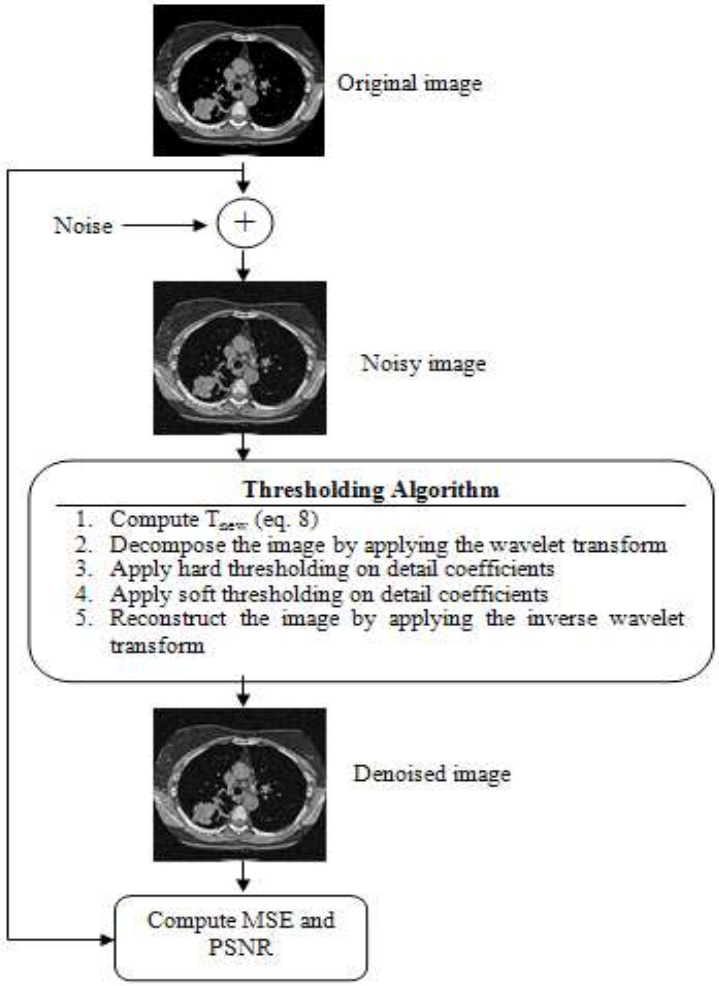

Fig.3 : Proposed denoising scheme

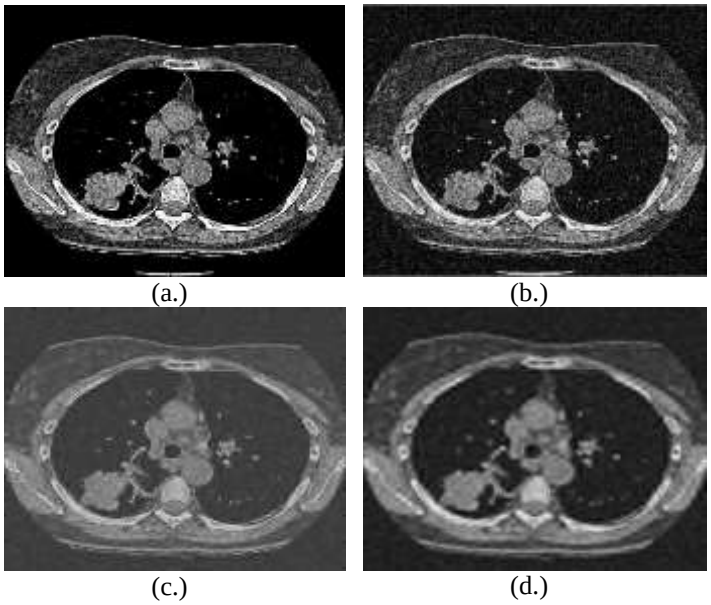

Fig. 4: (a) Original CT image (b) noisy image with σ = 50 (c) de-noised using hard thresholding with our proposed thresh, and (d) de-noised using soft thresholding with our proposed thresh

TABLE I. RESUSLTS OBTAINED FOR THE GAUSSIAN NOISE

Noise Levels	Wavelet	Wavelet level	Results (PSNR in dB)			
			Soft denoising		*Hard denoising*	
			T_{Donoho}	T_{new}	T_{Donoho}	T_{new}
10	Haar	2	21,43	23,32	24,86	**27,28**
	Haar	3	21,07	23,01	24,71	27,19
	Haar	4	20,93	22,89	24,68	27,17
	Db4	2	21,54	23,36	24,75	27,09
	Db4	3	21,12	23,00	24,55	26,96
	Db4	4	20,96	22,86	24,51	26,93
	Symlet 4	2	21,59	23,41	24,81	27,11
	Symlet 4	3	21,20	23,07	24,61	26,98
	Symlet 4	4	21,05	22,93	24,57	26,95
	Coifflet 4	2	21,60	**23,41**	24,82	**27,12**
	Coifflet 4	3	21,19	23,06	24,62	26,97
	Coifflet 4	4	21,04	22,92	24,56	26,94
20	Haar	2	18,47	19,68	20,17	21,84
	Haar	3	17,99	19,30	19,95	21,71
	Haar	4	17,77	19,12	19,90	21,67
	Db4	2	18,73	19,85	20,25	21,89
	Db4	3	18,18	19,41	19,98	21,71
	Db4	4	17,93	19,21	19,90	21,66
	Symlet 4	2	18,74	19,89	20,30	21,95
	Symlet 4	3	18,23	19,48	20,07	21,79
	Symlet 4	4	17,99	19,29	19,99	21,74
	Coifflet 4	2	18,77	**19,91**	20,33	**21,96**
	Coifflet 4	3	18,23	19,47	20,07	21,78
	Coifflet 4	4	17,99	19,29	19,98	21,73
30	Haar	2	17,24	18,03	18,23	19,40
	Haar	3	16,68	17,59	17,95	19,22
	Haar	4	16,38	17,37	17,85	19,18
	Db4	2	17,58	18,28	18,38	19,51
	Db4	3	16,93	17,78	18,03	19,29
	Db4	4	16,59	17,53	17,90	19,21
	Symlet 4	2	17,58	18,29	18,42	19,54
	Symlet 4	3	16,97	17,83	18,12	19,37
	Symlet 4	4	16,65	17,60	18,00	19,30
	Coifflet 4	2	17,61	**18,32**	18,41	**19,56**
	Coifflet 4	3	16,98	17,84	18,07	19,36
	Coifflet 4	4	16,66	17,60	17,95	19,29
50	Haar	2	16,03	16,32	16,28	16,93
	Haar	3	15,39	15,84	15,89	16,73
	Haar	4	14,95	15,52	15,71	16,63
	Db4	2	16,39	16,65	16,62	17,13
	Db4	3	15,70	16,10	16,16	16,86
	Db4	4	15,24	15,76	15,95	16,74
	Symlet 4	2	16,39	16,66	16,62	17,13
	Symlet 4	3	15,71	16,14	16,21	16,91
	Symlet 4	4	15,27	15,81	16,02	16,80
	Coifflet 4	2	16,42	**16,69**	16,65	**17,15**
	Coifflet 4	3	15,75	16,16	16,22	16,91
	Coifflet 4	4	15,32	15,83	16,01	16,78

TABLE II. RESUSLTS OBTAINED FOR THE SPECKLE NOISE

Noise Levels	Wavelet	Wavelet level	Results (PSNR in dB)			
			Soft denoising		*Hard denoising*	
			T_{Donoho}	T_{new}	T_{Donoho}	T_{new}
10	Haar	2	21,60	23,60	25,42	28,54
	Haar	3	21,23	23,27	25,23	28,39
	Haar	4	21,10	23,16	25,19	28,35
	Db4	2	21,71	23,63	25,28	28,25
	Db4	3	21,28	23,25	25,05	28,04
	Db4	4	21,12	23,12	24,99	27,99
	Symlet 4	2	21,76	23,68	25,35	28,27
	Symlet 4	3	21,35	23,31	25,10	28,06
	Symlet 4	4	21,21	23,19	25,05	28,01
	Coifflet 4	2	21,77	23,69	25,33	28,25
	Coifflet 4	3	21,35	23,31	25,09	28,04
	Coifflet 4	4	21,20	23,18	25,02	27,99
20	Haar	2	18,73	20,02	20,63	22,73
	Haar	3	18,22	19,59	20,35	22,52
	Haar	4	18,01	19,43	20,28	22,47
	Db4	2	18,99	20,20	20,70	22,73
	Db4	3	18,39	19,70	20,36	22,47
	Db4	4	18,15	19,51	20,27	22,40
	Symlet 4	2	19,01	20,24	20,77	22,82
	Symlet 4	3	18,46	19,78	20,47	22,56
	Symlet 4	4	18,23	19,60	20,38	22,50
	Coifflet 4	2	19,04	20,26	20,77	22,82
	Coifflet 4	3	18,46	19,78	20,43	22,55
	Coifflet 4	4	18,23	19,59	20,34	22,48
30	Haar	2	17,69	18,55	18,81	20,30
	Haar	3	17,05	18,03	18,42	20,02
	Haar	4	16,75	17,81	18,32	19,95
	Db4	2	18,04	18,82	18,99	20,39
	Db4	3	17,29	18,21	18,53	20,05
	Db4	4	16,96	17,96	18,39	19,96
	Symlet 4	2	18,04	18,84	19,01	20,47
	Symlet 4	3	17,34	18,28	18,61	20,17
	Symlet 4	4	17,02	18,04	18,48	20,07
	Coifflet 4	2	18,08	18,88	19,02	20,48
	Coifflet 4	3	17,35	18,28	18,59	20,15
	Coifflet 4	4	17,03	18,04	18,46	20,05
50	Haar	2	16,95	17,34	17,29	18,20
	Haar	3	16,09	16,65	16,72	17,79
	Haar	4	15,62	16,31	16,50	17,66
	Db4	2	17,40	17,73	17,72	18,44
	Db4	3	16,43	16,92	17,00	17,94
	Db4	4	15,91	16,54	16,75	17,77
	Symlet 4	2	17,40	17,73	17,74	18,43
	Symlet 4	3	16,45	16,97	17,08	18,00
	Symlet 4	4	15,96	16,60	16,85	17,84
	Coifflet 4	2	17,44	17,77	17,79	18,47
	Coifflet 4	3	16,48	16,98	17,10	17,98
	Coifflet 4	4	16,00	16,62	16,83	17,82

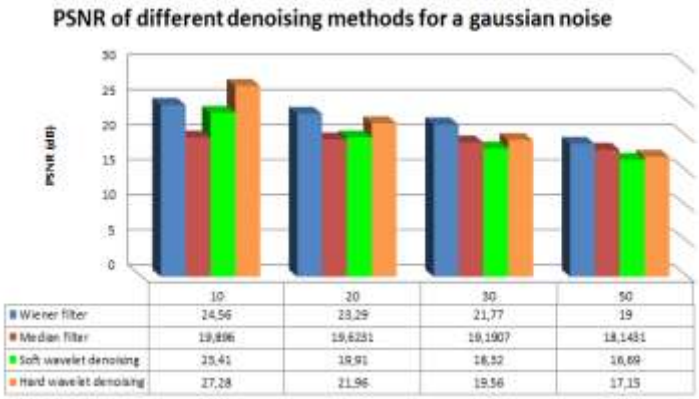

Fig. 5: Different denoising scheme for a Gaussian noise

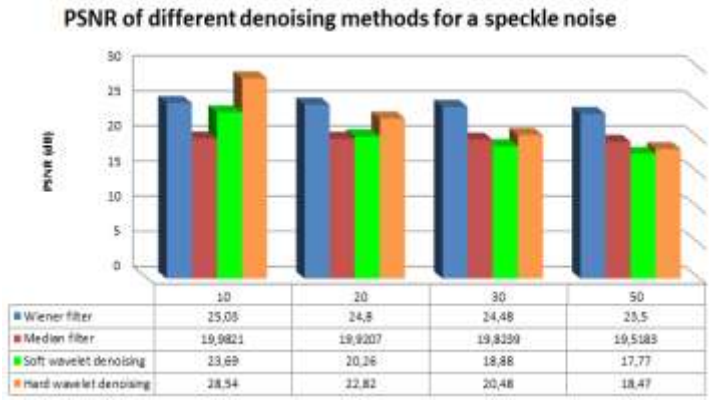

Fig. 6: Different denoising scheme for a Speckle noise

Table 3 gives an idea about the results obtained using wavelets for denoising CT lung images. The applied noses are Gaussian taken with two levels, 10 and 20. We can see that our results, in term of PSNR, are similar to those given by Bhadauria and Singh [2].

TABLE III. DIFFERENT RESULTS PRESENTED IN LITERATURE

	PSNR (db)		
	$\sigma = 10$	$\sigma = 20$	Used database
Results given in [2]	29.36	25.56	LIDC
Our results	27.12	21.96	ELCAP

V. CONCLUSION

In this paper, we have proposed a new denoising scheme that removes the noise significantly and performs the universal denoising scheme in terms of PSNR for all values of noise level. The comparative result shows that the proposed threshold value found to be better than universal threshold. The comparative PSNR value of the proposed threshold improves with increase in the noise level. In this sense our threshold value is an important contribution to the choice of the threshold to remove the noise from the image using wavelets.

ACKNOWLEDGMENT

We would like to thank Al BAHA University for supporting this work and providing the research funds.

REFERENCES

[1] Ali, S.-A., S. Vathsal, and L. Lal kishore, An Efficient Denoising Technique for CT Images using Windowbased Multi-Wavelet Transformation and Thresholding, European Journal of Scientific Research, Vol. 48, No. 2, pp. 315-325, 2010.

[2] Bhadauria, H.- S. and A. Singh, Wavelet and Canny Based Edge Detection Method for Noisy Lung CT Image, International Journal of Emerging Technology and Advanced Engineering, Vol. 3, No. 5, pp. 776-780, 2013.

[3] Deng, J. L. Haiyun, and Hao Wu, A CT Image Denoise Method Using Curvelet Transform, Communication Systems and Information Technology, Vol. 100, pp. 681-687, 2011.

[4] Donoho D.-L. and I.-M. Johnstone, Ideal Spatial Adaptation via Wavelet Shrinkage, Biometrika, Vol. 81, No. 3, pp. 425-455, 1994.

[5] Donoho D.-L, De-Noising by Soft-Thresholding, IEEE trans. On Information Theory, Vol. 41, No. 3, pp. 613-627, 1995.

[6] Donoho D.-L. and I.-M. Johnstone, Adapting to Unknown Smoothness via Wavelet Shrinkage," Journal of American Statistical Association, Vol. 90, No. 432, pp. 1200-1224, 1995.

[7] Dubey, S. and C.-A. Powell, Update in lung cancer 2008, Am. J. Respir. Crit. Care Med., Vol. 179, No. 10, pp. 860–868, 2009.

[8] Ferlay, J., I. Soerjomataram, M. Ervik, R. Dikshit, S. Eser, C. Mathers, M. Rebelo, D.M. Parkin, D., Forman and F. Bray, Cancer Incidence and Mortality Worldwide in 2012, Report of the International Agency for Research on Cancer, http:// globocan.iarc.fr.

[9] Garnavi, R., A. Baraani-Dastjerdi, H. Abrishami Moghaddam, M. Giti and A.-A. Rad, new segmentation method for lung HRCT images, In Proc. of the International Conference on Digital Image Computing: Techniques and Applications, DICTA '05, pp. 52, 2005.

[10] Gori, I., R. Bellotti and P. Cerello, Lung nodule detection in screening computed tomography, In Proc. of the IEEE Nuclear Science Symposium Conference Record, pp. 3489 – 3491, San Diego, 2006.

[11] Guo D.-f., W.-H. Zhu, Z.-M. Gao, and J.-Q. Zhang, A study of wavelet thresholding denoising, In Proc. of the 5th International Conference on Signal Processing WCCC-ICSP'2000, pp. 329-332, 2000.

[12] Gurcan, M.N., B. Sahiner, and N. Petrick, Lung nodule detection on thoracic computed tomography images: preliminary evaluation of a computer-aided diagnosis system. Med. Phys. Vol. 29, pp. 2552–2558, 2002.

[13] Joy J., S. Peter, and N. John, Denoising Using Soft Thresholding, International Journal of Advanced Research in Electrical, Electronics and Instrumentation Engineering, Vol. 2, pp. 1027-1031, 2013.

[14] Kim, H., T. Nakashima, and Y. Itai, Automatic detection of ground glass opacity from the thoracic MDCT images by using density features, In Proc. of the International Conference on Control, Automation and Systems, pp. 1274–1277, Seoul, 2007.

[15] Lee S.-L.-A., A.-Z Kouzani, and E.-J. Hu, Automated detection of lung nodules in computed tomography images: a review, Machine Vision and Applications, Vol. 23, pp. 151–163, 2012.

[16] Lin, D.-T. and C.-R Yan, Lung nodules identification rules extraction with neural fuzzy network, In proc of the 9th International Conference of Information Processing (ICONIP), Vol. 4, pp. 2049 – 2053, Singapore, 2002.

[17] Lin, D.-T., C.-R. Yan, and W.-T. Chen, Autonomous detection of pulmonary nodules on CT images with a neural network-based fuzzy system, Comput. Med. Imaging Graph. Vol. 29, pp. 447–458, 2005.

[18] Mahersia, H., L. Gabralla and M. Zaroug, Lung Cancer Detection on CT scan images: A Review on the analysis Techniques, International Journal of Advanced Research in Artificial Intelligence, Vol. 4, No. 4, pp. 38-45, April 2015.

[19] Mahersia, H., K. Hamrouni, and N. Ellouze, Wavelet texture analysis and fuzzy C-mean classification for image segmentation, In Proc. of the 9th Maghrebian Conference on Information Technologie MCSEAI'06, Agadir, Maroc, 2006.

[20] Pu, J., J. Roos, and C.-A. Yi, Adaptive border marching algorithm: automatic lung segmentation on chest CT images, Comput. Med. Imaging Graph., Vol. 32, pp. 452–462, 2008.

[21] Retico, A., P. Delogu, and M.-E. Fantacci, Lung nodule detection in low-dose and thin-slice computed tomography, Comput. Biol. Med., Vol. 38, pp. 525–534, 2008.

[22] Senthil-Kumar T.-K. and E.-N. Ganesh, Proposed Technique for Accurate Detection/Segmentation of Lung Nodules using Spline Wavelet Techniques, Int J Biomed Sci., Vol. 9, No. 1, pp. 9–17, 2013.

[23] Vijaya G. and A. Suhasini, An Adaptive Preprocessing of Lung CT Images with Various Filters for Better Enhancement, Academic Journal of Cancer Research, Vol. 7, No. 3, pp. 179-184, 2014.

[24] Wei, G.-Q., L. Fan and J. Qian, Automatic detection of nodules attached to vessels in lung CT by volume projection analysis, Medical Image Computing and Computer-assisted Intervention, MICCAI, Vol. 2488, pp. 746–752, 2002.